Early Lipofuscin Accumulation in Frontal Lobe Epilepsy

Joan Y.W. Liu, PhD,[1,2] Cheryl Reeves, PhD,[1,2] Beate Diehl, MD, PhD, FRCP,[2,3] Antonietta Coppola, MD, PhD,[2] Aliya Al-Hajri, MD,[4] Chandrashekar Hoskote, MD,[4] Salim al Mughairy, MD, FRCR,[4] Mohamed Tachrount, PhD,[4] Michael Groves, PhD,[1] Zuzanna Michalak, PhD,[1,2] Kevin Mills, PhD,[5] Andrew W. McEvoy, MD, FRCS, SN,[2,6] Anna Miserocchi, MD,[6] Sanjay M. Sisodiya, MD, PhD, FRCP, FRCPE,[2,7] and Maria Thom, MD, MRCPath[1,2]

Objective: This study reports on a novel brain pathology in young patients with frontal lobe epilepsy (FLE) that is distinct from focal cortical dysplasia (FCD).
Methods: Surgical specimens from 20 young adults with FLE (mean age, 30 years) were investigated with histological/immunohistochemical markers for cortical laminar architecture, mammalian target of (mTOR) pathway activation and inhibition, cellular autophagy, and synaptic vesicle-mediated trafficking as well as proteomics analysis. Findings were correlated with pre-/postoperative clinical, imaging, and electrophysiological data.
Results: Excessive lipofuscin accumulation was observed in abnormal dysmorphic neurones in 6 cases, but not in seven FCD type IIB and 7 pathology-negative cases, despite similar age and seizure histories. Abnormal dysmorphic neurones on proteomics analysis were comparable to aged human brains. The mTOR pathway was activated, as in cases with dysplasia, but the immunoreactivities of nucleoporin p62, DEP-domain containing protein 5, clathrin, and dynamin-1 were different between groups, suggesting that enhanced autophagy flux and abnormal synaptic vesicle trafficking contribute to early lipofuscin aggregation in these cases, compared to suppression of autophagy in cases with typical dysplasia. Cases with abnormal neuronal lipofuscin showed subtle magnetic resonance imaging cortical abnormalities that localized with seizure onset zone and were more likely to have a family history.
Interpretation: We propose that excess neuronal lipofuscin accumulation in young patients with FLE represents a novel pathology underlying this epilepsy; the early accumulation of lipofuscin may be disease driven, secondary to as-yet unidentified drivers accelerating autophagic pathways, which may underpin the neuronal dysfunction in this condition.

ANN NEUROL 2016;00:000–000

The cause of focal epilepsy syndromes, including frontal lobe epilepsies (FLEs), is being regularly advanced through clinical, genetic, and pathological studies.[1] Novel gene mutations have been recently identified; for example, *DEPDC5* mutations are associated with familial FLE syndromes (familial focal epilepsy with variable foci[1,2] as well as cases of sporadic FLE and with pathologically proven focal cortical dysplasia (FCD).[3–5] Historically, studies of histologically defined malformations of cortical development in symptomatic epilepsies have significantly advanced identification of specific genetic defects and causative cellular pathways.[6,7] FCD is a cortical

View this article online at wileyonlinelibrary.com. DOI: 10.1002/ana.24803

Received Apr 22, 2016, and in revised form Oct 17, 2016. Accepted for publication Oct 17, 2016.

Address correspondence to Prof Maria Thom, Division of Neuropathology and Department of Clinical and Experimental Epilepsy, 1st Floor Queen Square House, UCL Institute of Neurology, Queen Square, London, WC1N 3BG, United Kingdom. E-mail: m.thom@ucl.ac.uk

From the [1]Division of Neuropathology, National Hospital for Neurology and Neurosurgery, London, United Kingdom; [2]Department of Clinical and Experimental Epilepsy, UCL Institute of Neurology, London, United Kingdom; [3]Department of Clinical Neurophysiology, National Hospital for Neurology and Neurosurgery, London, United Kingdom; [4]The Lysholm Department of Neuroradiology in National Hospital for Neurology and Neurosurgery, London, United Kingdom and Department of Brain Repair and Rehabilitation, UCL Institute of Neurology, London, UK; [5]Biological Mass Spectrometry Centre, Institute of Child Health, University College London, London, United Kingdom; [6]Victor Horsley Department of Neurosurgery, National Hospital for Neurology and Neurosurgery, London, United Kingdom; and [7]Epilepsy Society, Chesham Lane, Chalfont St Peter, United Kingdom

Additional supporting information can be found in the online version of this article.

malformation first recognized in an epilepsy surgical pathology series in 1971[8] and is now the commonest histologically confirmed malformation, with a predilection for the frontal lobe.[9] Although FCD mainly occurs sporadically, somatic or germline mutations in mammalian target of rapamycin (mTOR) pathway genes have now been reported by several groups.[10–12]

There are currently nine subtypes of FCD, defined by their pathological characteristics of cytoarchitectural and associated abnormalities.[13] FCD type II (FCDII) is the best-defined subtype, characterized by dysmorphic neurones (FCDII type A; FCDIIA) and balloon cells (FCDII type B; FCDIIB). FCDIIB is generally associated with favorable outcome following surgical resection,[9] particularly when lesions are well defined on magnetic resonance (MR) imaging (MRI) and fully resected, with seizure-free outcomes as high as 75%[14] to 87.5%.[15] Multimodal investigation integrating neuroimaging, electrophysiological, and functional studies is advocated in the surgical planning of patients with focal epilepsies, including suspected FCD.[9] However, classical imaging features are not always present in FLE resections.

In this study of patients with FLE, we present evidence for a novel and distinct neuronal pathology, characterized by excessive lipofuscin accumulation in dysmorphic neurones. We hypothesized a primary abnormality in autophagy and compared multimodal investigations, including neuroimaging, electrophysiology, proteome, mTOR, and autophagic pathway analysis, to highlight the distinct characteristics of this pathology and determine the possible pathomechanism underlying this pathology.

Patients and Methods

Case Selection and Clinical Investigations

Twenty patients operated on over a 5-year period (2009–2013) who had undergone surgical resections as a treatment of focal drug-resistant FLE were identified from the records of the UCL Epilepsy Society Brain and Tissue Bank (Supplementary Table 1). Surgical tissue was consented for use in research, and the study has ethical approval (National Research Ethics Service 12/SC/0669). Cases with vascular malformations and tumors were excluded. Clinical records of patients, including their epilepsy history, family history, and psychometry, were reviewed. Preoperative brain MRI and positron emission tomography, electroencephalography (EEG), videotelemetry, psychometry, functional imaging, and intracranial EEG (IC-EEG) studies had been carried out according to the epilepsy surgical protocols at the National Hospital of Neurology and Neurosurgery and were reviewed in each case.

All patients were studied on the 3 Tesla (T) MRI scanner at the Epilepsy Society, Chalfont, UK. The MR protocol included T1-weighted, T2-weighted, and fluid-attenuated immersion recovery images using the standard epilepsy protocol for presurgical evaluation.[16] In all cases, strategies for implantation of subdural grids and/or depth electrodes were agreed at a multidisciplinary meeting and were carried out using methodologies, as previously reported.[17] In all patients studied, a putative epileptogenic zone was identified, and patients proceeded to resection of frontal lobe cortex and white matter, tailored according to integrated EEG, imaging, and functional imaging findings (Supplementary Table 1).

Neuropathology

Between two and five surgical samples were received from each case according to regions of differing ictal activity on IC-EEG and lesional abnormality if defined on MRI (Supplementary Table 1). Fresh specimens were orientated for photography, sliced, and, where available, samples of normal and macroscopically abnormal fresh tissues were snap frozen using liquid nitrogen. The remaining specimens were fixed in formalin for 24 hours and then further cut into 5-mm-thick tissue blocks. Histological and immunohistochemical investigations were then performed on all tissue blocks using methods as published in previous studies[18] (Supplementary Table 2). Immunolabelling was assessed qualitatively using a bright-field microscope (Nikon Eclipse 80i; Nikon Instruments, Tokyo, Japan). For the detection of autofluorescence, one 5-μm-thin section from each case was washed in phosphate-buffer solution for 5 minutes after xylene and alcohol immersions. Sections were then coverslipped using 4',6-diamidino-2-phenylindole containing mounting medium (Vector Laboratories Inc., Peterborough, UK). Autofluorescence was visualized using a fluorescent microscope with excitation wavelength at 470nm and detection at 520nm (Carl Zeiss Microscopy, LLC, Thornwood, NY).

Electron Microscopy

Electron microscopy (EM) was performed on 2 cases with abnormal neurones on periodic acid–Schiff (PAS) stain. Because abnormal cells were often only focally present in the tissue section, these abnormal regions were dissected from regions identified from the formalin-fixed, paraffin-embedded tissue blocks, processed for EM, and examined with a Philips CM10 electron microscope (Philips Electron Optics, Eindhoven, The Netherlands) and images acquired using a Megaview III digital camera and analySIS iTEM software (Olympus Soft-Imaging Solutions Corp., Lakewood, CO).

Proteomics

Frozen cortical samples from 5 selected cases (cases E1, E2, E8, E13, and E19) were processed for proteomic analysis. For each case, 10 sections of 14-μm thickness were cut on the cryostat and collected onto polyethylene terephthalate metal frame slides for laser capture microdissection (Leica, Milton Keynes, UK). One additional section was collected onto a microscopic slide (VWR International, Leicestershire, UK) and stained briefly in 0.1% toluidine blue (pH 4.5) solution for 5 seconds to identify the region of interest (ROI). Laser capture microdissection (LCM 700; Leica) was then carried out on the ROI of multiple

sections per case to include abnormal, dysmorphic neurones in cases with excess focal neuronal lipofuscin (FNL) and those with FCDIIB, and neurones in pathology-negative cases until a total tissue area of 8 to 8.6mm^2 had been dissected and collected in a 0.5-ml Eppendorf tube (VWR International).

Dissected samples were denatured using in-solution trypsin digestion and prepared for MSe label-free quantitative proteomics, as described previously.[19] Peptide identification was accepted if they could be established at 95% or greater probability. Quantity of proteins extracted was normalized against the total protein of each sample (fmol/ng) and then these values were compared between cases with FNL, pathology-negative, and FCBIIB cases using bioinformatics resources, DAVID (version 6.7), Ingenuity Pathway Analysis (Qiagen, Manchester, UK), and ConsensusPathDB (version 31). *p* values and adjusted *p* values (corrected according to Bonferroni's method and false discovery rate) were calculated by bioinformatics resources. For gene ontology annotation and enriched pathway analyses, the *p* value cutoff was set at 0.01, and only pathways with four or more proteins of interest were highlighted.

Results

Of the 20 cases with FLE included this study (Supplementary Table 1), 6 (E1–E6) showed the specific pathology we term *focal neuronal lipofuscinosis* (FNL). These cases were characterized by the presence of hypertrophic, pyramidal, or globoid cortical neurones resembling dysmorphic neurones (Fig 1A–P). The cytoplasm of these neurones was markedly distended and ballooned with granular material on hematoxylin-eosin (H&E; Fig 1B) that was both PAS and Sudan Black positive, and autofluoresced at an excitation wavelength of 470nm (Fig 1C–E,P) consistent with neuronal lipofuscin.[20,21] This abnormal storage material extended to the axon hillock in some dysmorphic neurons (Fig 1C,E, arrows). We termed these cells dysmorphic neurones with excess lipofuscin (DN/L). The enlarged perikarya and abnormal dendritic polarity of DN/L were highlighted by nonphosphorylated neurofilament stains (SMI32), which showed intense labeling of cytoplasmic filaments marginalized to the periphery of the neurone, producing "ring-like" structures (Fig 1F,L,N). Combined PAS/SMI32 staining showed the location of the central granular, cytoplasmic PAS staining within peripherally arranged neurofilaments (Fig 1G). All PAS-distended neurones had strong labeling with antineurofilament antibodies. There were also interspersed normal-sized neurones with weak PAS cytoplasmic granular positivity, but without abnormal neurofilament distribution. Phosphorylated neurofilament (SMI31) was expressed in fewer DN/L than labeled with the SMI32 antibody, but a similar ring-like cellular pattern was still observed (Fig 1L, right). DN/L were distributed across all cortical layers (E1, E3) or predominated in the deeper cortical layers (E2, E4–E6), but DN/L were not present in the white matter. In cases E1 and E3, a six-layered cortical architecture was indistinct (Figs 1A and 5L), whereas in other cases, as well as at the margins, DN/L appeared scattered in cortex with relatively preserved lamination. In case E3, DN/L were localized to the depth of one sulcus (Fig 5J–L). Regions populated by DN/L were more extensive and readily evident on H&E-stained sections in cases E1 to E3 compared to cases E4 to E6, where changes were more subtle with scattered, less-frequent DN/L (Supplementary Table 1).

CD34, calbindin, and nestin markers did not label DN/L. In all 6 cases, glial fibrillary acidic protein labeling revealed a reactive superficial, or Chaslin's type, gliosis. No balloon cells were present. White matter and cortical myelination patterns were normal, as shown on myelin basic protein (SMI94) immunolabeling. Iba1 and CD68 immunolabeling revealed a mild upregulation of microglia in the regions with DN/L and inflammatory foci in relation to electrode track sites only. We did not observe any relationship between the electrode track injury sites and the cortex populated by DN/L (Supplementary Table 1). Focal, granular ubiquitin immunoreactivity was observed in a minority of cells in 4 cases with DN/L (E1–E3 and E5; Fig 1H,O). Granular p62 cytoplasmic immunolabeling was only observed in cases E1 and E5 (Fig 1I), with some skein-like filamentous material noted in case E1 (Fig 1I, inset). There was no AT8 labeling in any case. Immunohistochemistry using two anti-pS6 antibodies revealed intense cytoplasmic labeling in the majority of DN/L, especially when compared to adjacent or intervening normally sized, normally labeled neurones (Fig 1J,K). DEPDC5 immunohistochemistry did not show evidence for strong labeling of DN/L compared to adjacent or intervening normal cortical neurones or glia (Fig 1K, inset). EM was carried out on cases E1 and E2. In these sections, electron-dense deposits were observed filling the cytoplasm, associated with lipid and compatible with lipofuscin (Fig 1M).

In comparison to cases with FNL, no specific neuropathology was identified in the frontal lobe samples of 7 cases (E7–E13; pathology negative). Small amounts of PAS-positive cytoplasmic granules were observed in occasional neurons of these 7 cases, but no abnormal storage material was observed in DN or balloon cells using any of the stains, and cortical lamination was normal on neuronal nuclei (NeuN)-immunopositive sections. Inflammatory foci near sites of electrode track placements were noted. In 1 patient (E17), there was a small region of gliosis, possibly compatible with a previous traumatic lesion, but no definite contusion. Ubiquitin and p62

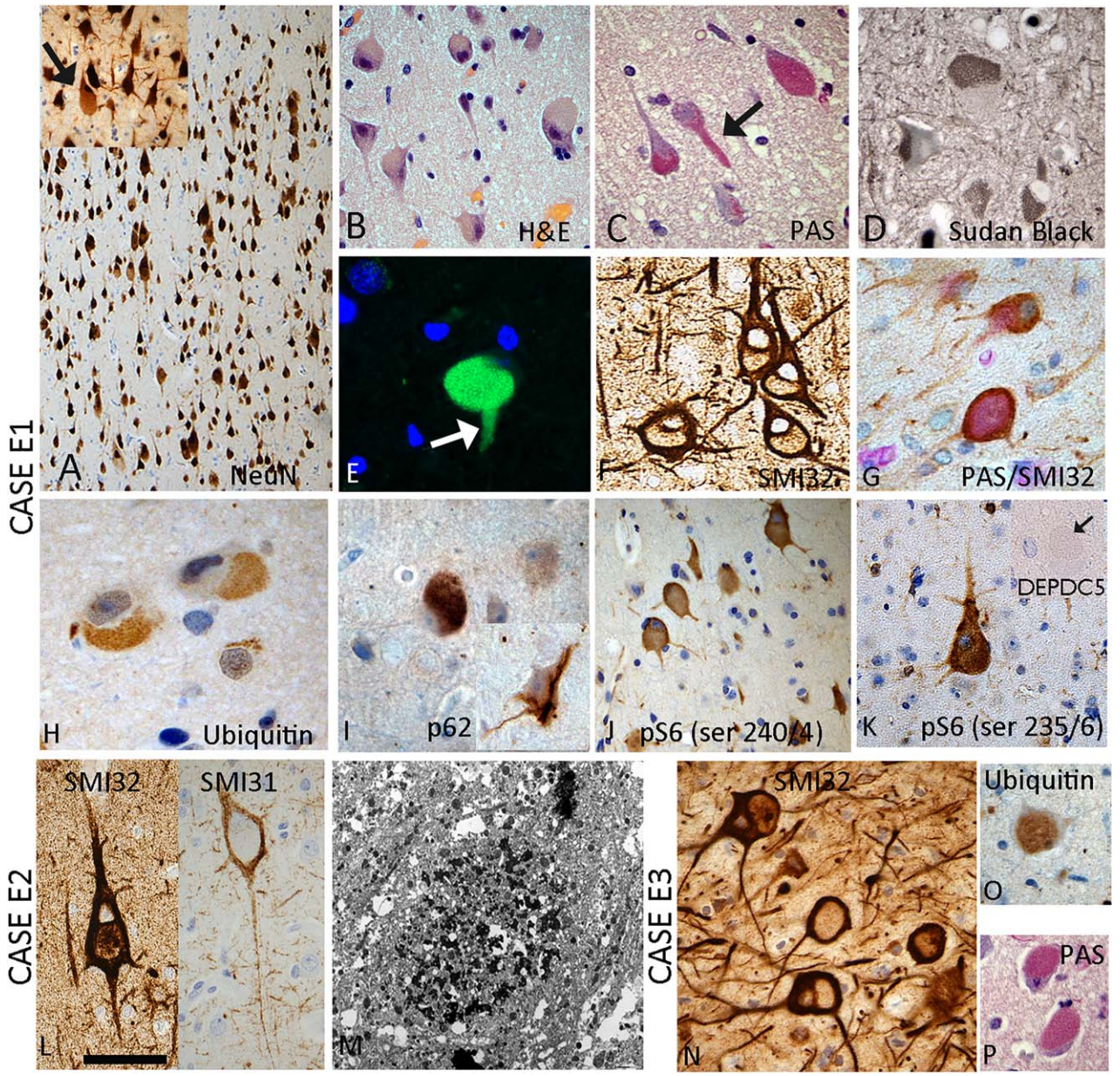

FIGURE 1: Frontal lobe epilepsy with focal neuronal lipofuscinosis (FNL). Case E1 (A–K), case E2 (L,M), and case E3 (N–P) (A) Enlarged, dysmorphic neurones were found throughout the cortical layers of case E1, highlighted with Neuronal Nuclei (NeuN) staining. They were intermingled with cortical neurones of more normal size; at higher magnification (shown in inset) cytoplasmic material was visible, distending the cytoplasm (arrowed). (B) On hematoxylin-eosin (H&E) stains, distended neuronal cells with accumulation of pale, cytoplasmic granular material, which was (C) periodic acid–Schiff (PAS) and (D) Sudan Black positive, and extended into the distended axon hillock (arrowed), was evident. (E) Distinct autofluorescence of the cytoplasm was also noted in this cell with material that extended into the axon hillock (arrow). (F) Neurofilament stain showed a distinct "ring-like" pattern of marginalised cytoplasmic neurofilaments. (G) Colocalization of the PAS-positive storage material in these abnormal ring-like dysmorphic neurones was confirmed through combined PAS and neurofilament (SMI32) staining. (H) Occasional neurones were positive for ubiquitin and (I) p62, but this was a less-consistent finding. (J,K) Immunolabeling, using pS6 as a marker of mammalian target of rapamycin pathway activation, consistently demonstrated pS6-immunopositive expression in dysmorphic neurones in this pathology, whereas DEPDC5 immunolabeling did not show evidence for obvious increased expression in dysmorphic neurones with excess lipofuscin (DN/L) compared to adjacent cortex and neurones or in comparison to other pathologies (arrow indicates a DN/L in the same case). (L) In case E2, DN/L were highlighted with both phosphorylated (SMI32) and nonphosphorylated neurofilament (SMI31) antibodies, both showing a ring-like peripheral labeling pattern surrounding the storage material. (M) Electron microscopy confirmed electron-dense, non-membrane-bound, cytoplasmic aggregates with the characteristic appearances of lipofuscin. (N) DN/L highlighted by neurofilament stains in case E3 with focal, weak ubiquitin labeling (O) and cytoplasmic PAS positivity (P). Scale bar equivalent to approximately 150 microns in (A), 50 microns in (B–D), (J,K), and 30 microns in (F–I), (L), (N–P), and 5 microns in (M).

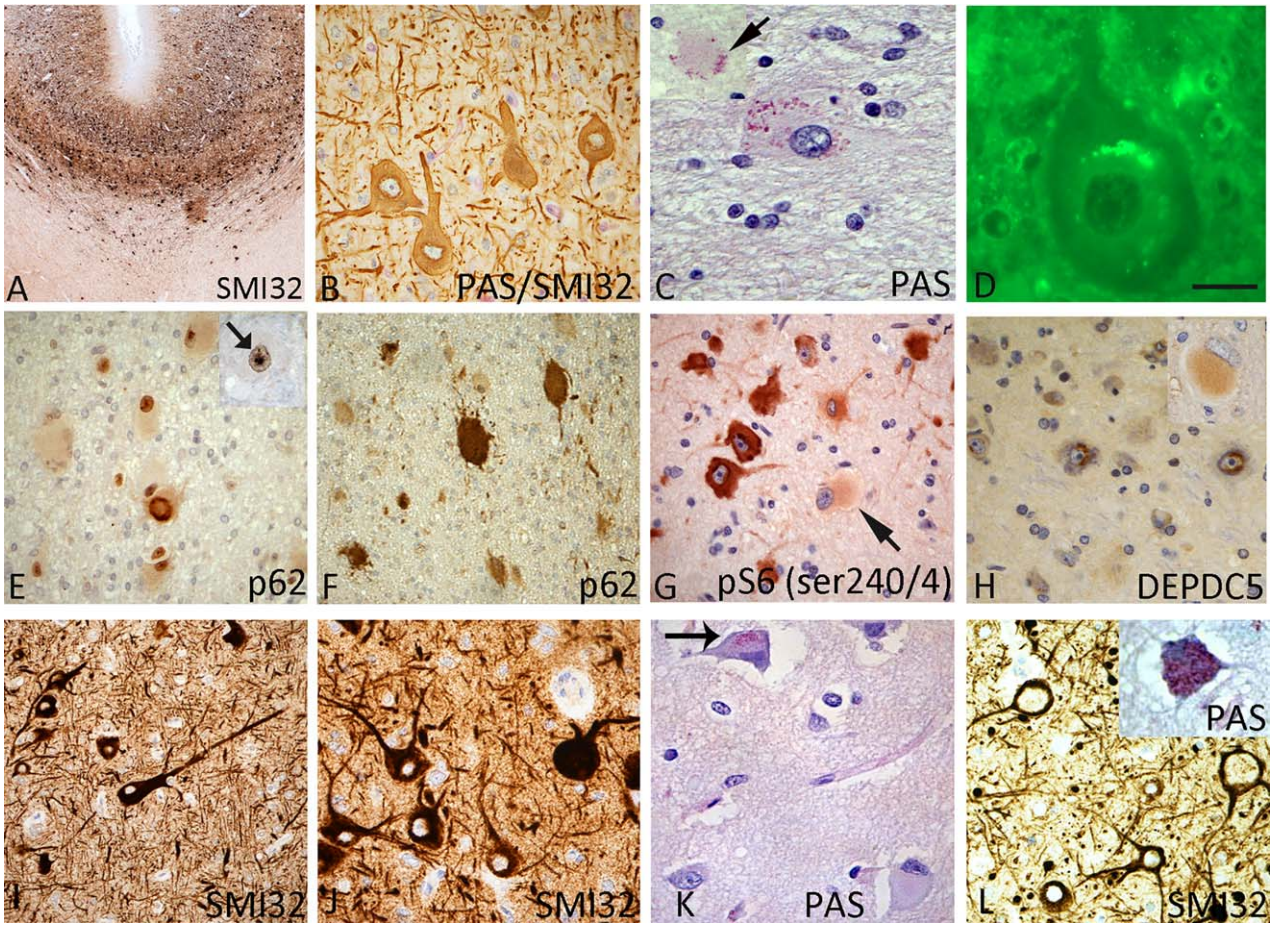

FIGURE 2: Immunoprofile of dysmorphic cells in frontal cortial dysplasia type IIB (FCDIIB). (A) FCBIIB (case E19) involving the depth of a sulcus with dysmorphic neurones (DN) populating the cortex and spilling into the underlying white matter (neurofilament stain, SMI32). (B) Unlike dysmorphic neurones with lipofuscin (DN/L) in frontal lobe epilepsy (FLE) with neuronal lipofuscin (FNL), DN in FCDIIB do not display marginalized neurofilaments or "ring cells" and there is no excess periodic acid–Schiff (PAS)-positive storage material in neurones. (C) A proportion of balloon cells showed scattered PAS-positive granules, more prominent in the periphery of some cells (inset, arrowed). (D) DN showed little autofluorescent cytoplasmic material. (E) Balloon cells in FCDIIB cases showed nuclear p62 immunopositivity and, in some cells, distinct intranuclear inclusions were noted (inset, arrowed) or (F) intense cytoplasmic labeling of balloon cells was observed. (G) pS6 immunohistochemistry showed strong cytoplasmic labeling of DN with generally weaker labeling of balloon cells (arrow). (H) Immunohistochemistry for DEPDC5 showed an intense paranuclear staining pattern in DN of FCDIIB, which was not noted in FNL or normal-appearing neurones in (FLE) cases; in addition, weaker cytoplasmic labeling of balloon cells was noted (insert). (I) FCDIIA involving the occipital lobe with SMI32 highlighting DN with intense labeling of neurofilament in the cytoplasm, but no ring-like cells are observed as consistently noted in FNL. This sample was processed in entirety, and no balloon cells were identified. (J) Another FCDIIA case involving the occipital lobe observed similar findings with intense SMI32-immunopositive labeling in the cell body and dendritic processes of DN. (K) PAS staining in FCDIIA cases showed, at the most, small accumulations of PAS-positive granules in the cytoplasm of a proportion of DN. (L) A cortical biopsy from a patient with a neurodegenerative condition and epilepsy with genetically confirmed Niemann-Pick type C. In the inset, cortical neurons showed cell bodies distended with weakly PAS-positive granular storage material, and prominent ring-like neurons were observed with neurofilament stains (SMI32), reminiscent of the pattern noted in FNL cases. Scale bar in (D) is equivalent to approximately 120 microns in (A), 50 microns in (B), (E,F), (G,H), and (I–L), and 30 microns in (C).

labeling revealed no specific labeling, except in case E11, where skein-like filamentous neuronal inclusions were observed. pS6-immunolabeled pyramidal and glial cells were occasionally scattered throughout the cortex of all cases, as previously described.[18] DEPDC5 did not show any distinct immunolabeling of neurones or glia, with only focal weak labeling of scattered pyramidal cells.

The remaining 7 cases in the series (E14–E20) showed typical pathology of FCDIIB, with DN in the cortex (Fig 2A) and hypomyelination of the underlying white matter with balloon cells. Neurofilament (SMI32) labeling did not reveal DN with ring-like expression of neurofilaments (Fig 2B) as observed in DN/L of cases with FNL. DN in FCDIIB cases did not have excess neuronal storage material, or excess PAS- or Sudan

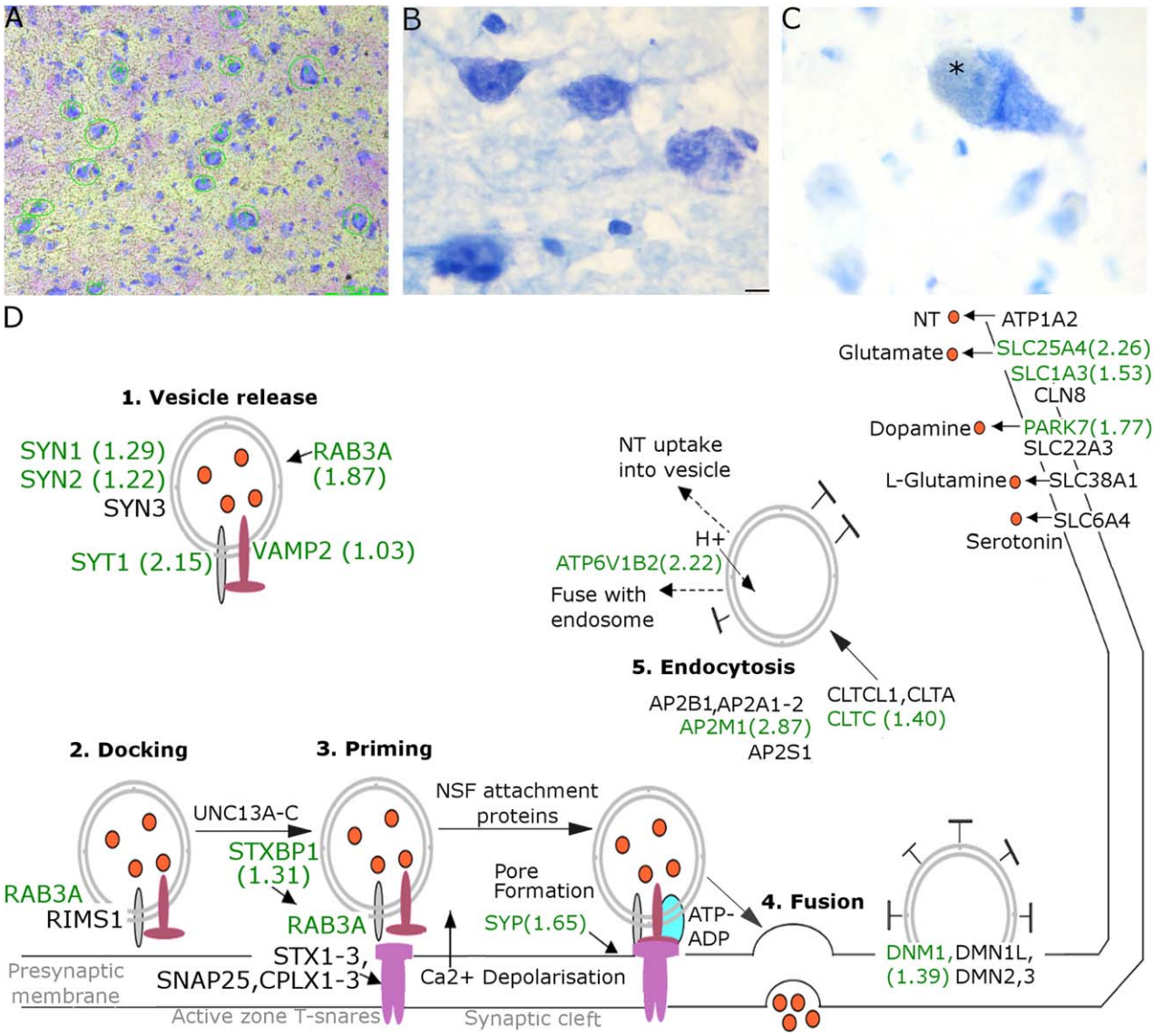

FIGURE 3: Proteomic analysis of dysmorphic neurones with lipofuscin (DN/L) (A) Neurones selected for laser capture microdissection were initially outlined (green). Images showing normal-appearing neurones of a pathology-negative case (B) and DN/L (C) of a frontal lobe epilepsy case with excess neuronal lipofuscin (asterisk; FNL) that were captured during laser microdissection. (D) Sixteen of the upregulated proteins in FNL cases (green) are involved in pathways associated with synaptic vesicles ($p < 0.001$; adjusted $p = 0.004$). Four of these proteins (clathrin, dynamin, syntaxin binding protein, and vesicle-associated membrane protein 2) had been described in a previous study investigating the proteome of lipofuscin in aged and Alzheimer's-diseased human brains (Ottis et al, 2012). At the presynaptic terminal of neurones, synaptic vesicles are actively loaded with neurotransmitters (NT) and then they are docked and "primed" at the "active zone" of the plasma membrane. When action potential arrives and depolarisation occurs, NT are released by exocytosis (fusion). Vesicles are retrieved through endocytosis. Diagram is adapted from WikiPathways.org (Pathway: WP2267) and Kyoto Encyclopaedia of Genes and Genomes (KEGG). Genes and proteins in (D) are as follow: AP2M1 = AP2 complex subunit mu; ATP6V1B2 = ATPase, H + transporting lysosomal 56/58kDa, V1 subunit B2; ATP6V1A = ATPase, H + transporting, lysosomal 70-kDa V1 subunit A; CLTC = clathrin heavy chain 1; DNM1 = dynamin 1.39; RAB3A = Ras-related protein Rab 3A; PARK7 = protein DJ 1 (Parkinson protein 7); RIMS1 = regulating synaptic membrane exocytosis 1; SLC1A3 = excitatory amino acid transporter 1; SLC25A4 = adenosine diphosphate (ADP) adenosine triphosphate (ATP) translocase 1; SNAP = synaptosomal-associated protein; STX = syntaxin; STXBP1 = synatxin binding protein 1; SYN = synapsin; SYP = synaptophysin; SYT1 = synaptotagmin 1. Numbers in brackets refer to fold increase of proteins in DN/L of FNL compared to pathology-negative cases. Scale bar in (B) and (C) = 10 μm. NSF = N-ethylmaleimide-sensitive factor.

Black–positive material, and showed minimal autofluorescence (Fig 2B–D). A few balloon cells in FCDIIB cases showed some fine granular PAS-positive staining in the cytoplasm (Fig 2C) or sometimes at the margins of the cell (Fig 2C, inset), reminiscent of the patterns reported in the cell culture of balloon cells, with accumulation of dense core lysosomes.[22] Balloon cells in FCDIIB cases also showed p62 immunopositivity, displaying both

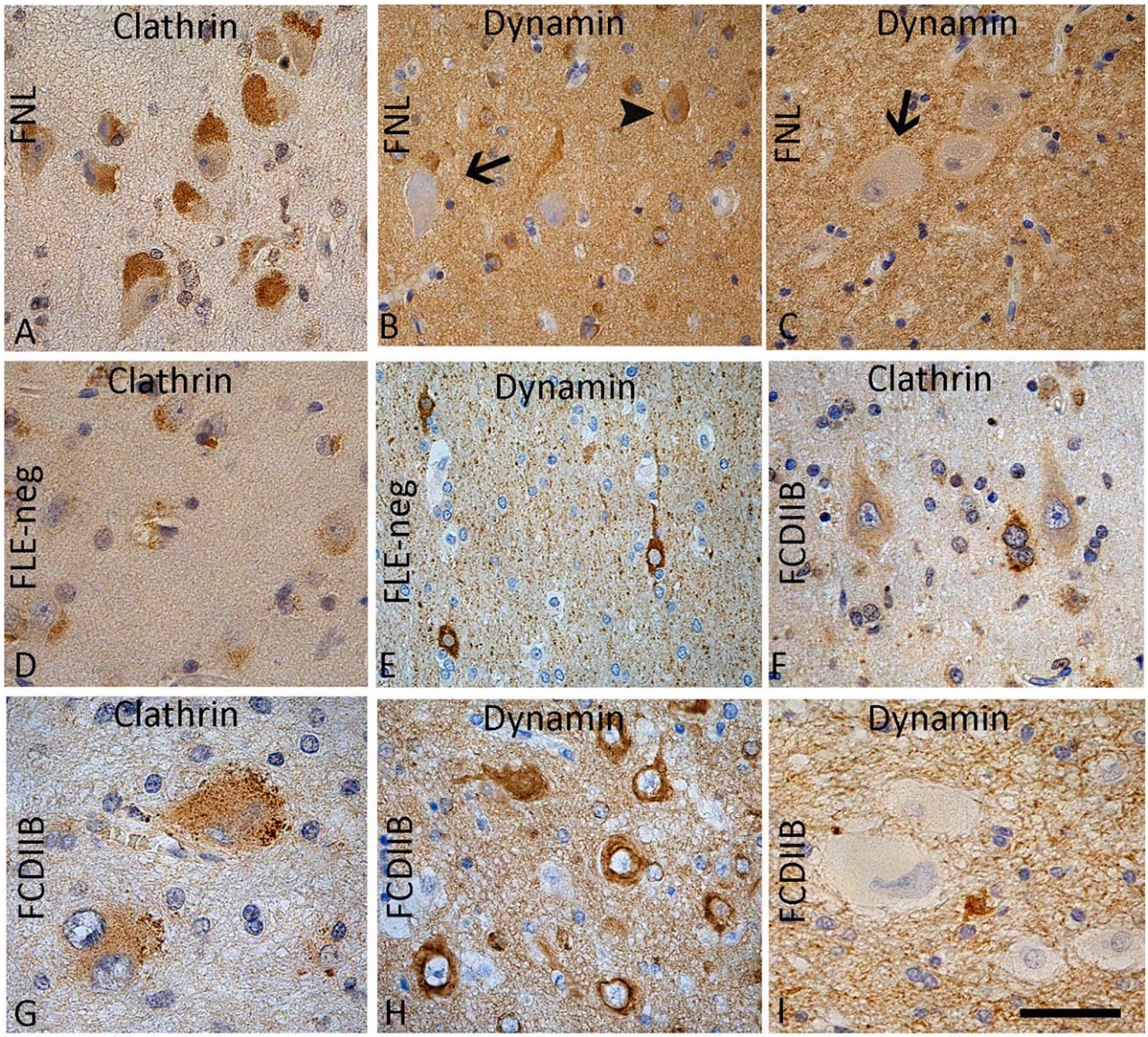

FIGURE 4: Clathrin and dynamin-1 immunohistochemistry in frontal lobe epilepsy (FLE) pathologies. (A) Cytoplasmic storage material in the dysmorphic neurones of FLE cases with excess neuronal lipofuscin (FNL) was strongly immunopositive for clathrin. (B,C) Most dysmorphic neurones with excess lipofuscin (DN/L) in FNL also expressed dynamin-1 in the cytoplasm, to a variable extent and intensity (arrowhead), but a proportion of neurones were distinctively dynamin-1 negative, as shown (arrows) in cases E1 (B) and E3 (C). (D) In pathology-negative FLE resections, small amounts of weakly clathrin-positive cytoplasmic granular material was noted in neurones, but intense labeling for dynamin-1, as illustrated in (E), in normal white matter interstitial neurones. (F) Sparse labeling of clathrin was observed in the dysmorphic neurones (DN) of FCDIIB although (G) more-consistent labeling of balloon cells with a peripheral granular pattern was noted. (H) Dynamin-1 immunohistochemistry typically showed intense cytoplasmic labeling of DN in FCDIIB, but (I) a striking lack of labeling of balloon cells was apparent. Scale bar in (A–F) and (H) is equivalent to 50 microns and (G) and (I) to approximately 30 microns.

nuclear (Fig 2E) and intense cytoplasmic labeling patterns (Fig 2F) with dot-like intranuclear p62 inclusions noted (Fig 2E, inset). In case E14, p62-positive DN were also observed. Ubiquitin immunoreactivity was not observed in balloon cells or DN. No tangles or AT8 immunolabeling were observed in any of the cases. pS6 immunohistochemistry showed intensely labeled DN compared to balloon cells (Fig 2G), as previously noted.[18] Prominent paranuclear aggregates with DEPDC5 were noted in the DN (Fig 2H), with some cytoplasmic labeling as well as variable cytoplasmic granular staining of balloon cells (Fig 2H, inset) with occasional intranuclear dot-like inclusions.

None of the cases in this series showed typical FCDIIA pathology.[13] Three archival FCDIIA cases from different cortical regions (Fig 2I–K) were reviewed for comparison to FNL. No DN/L were observed in any of the cases, although intense SMI32-immunopositive enlarged neurones were present.

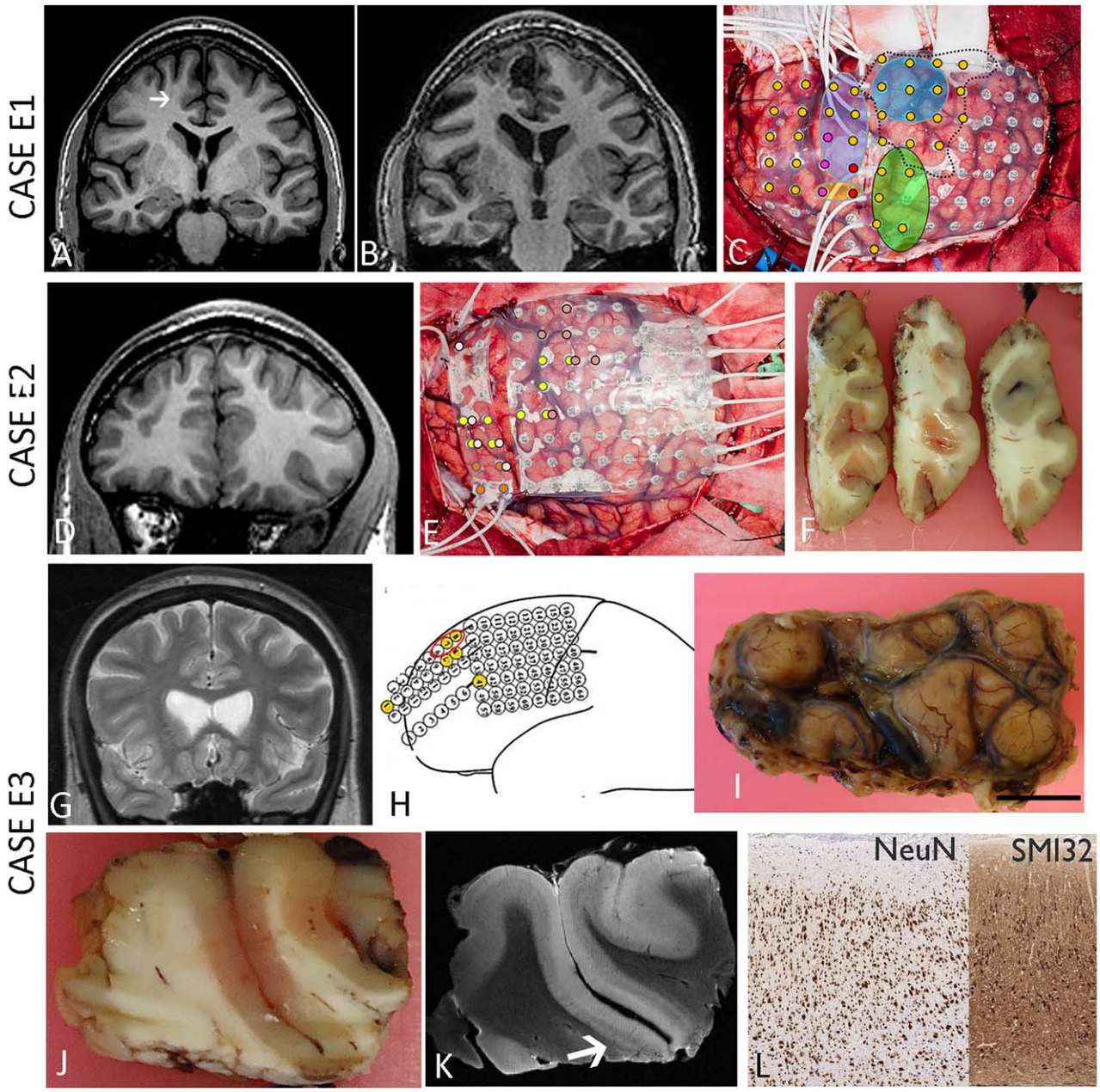

FIGURE 5: Clinical investigations in cases with frontal lobe epilepsy case with excess neuronal lipofuscin (FNL). Case E1 (A–C). Magnetic resonance (MR) imaging (MRI): A subtle area of blurring in the right frontal gray matter was noted on T1-weighted images preoperatively (A); the corresponding postoperative resection cavity is noted in (B). (C) Position of intracranial grids overlying the frontal cortex is marked with a dashed line showing the approximate area of the right frontal lobe for planned surgical resection, sparing the primary motor cortex. Oval areas demarcate the following functional fields: purple oval (primary motor); blue oval (front eye field); and green oval (face motor). Red circles indicate ictal onset, pink circles early spread within 1 second, and orange circles late spread within 1.5 to 2 seconds. Case E2 (D–F); (D) MRI T1-weighted coronal image showed no abnormality. (E) Electroencephalography (EEG) studies with grid in place; contact points involved in seizure activity are indicated as dark pink circles and late evolving regions after 50 seconds as pale pink circles; regions with interictal spikes (orange circles, higher amplitude; yellow circles, lower amplitude) are also shown. (F) Resected frontal lobe specimen was macroscopically normal following fixation and slicing at 5-mm intervals. (G) Case E3 (G–L): MRI T2-weighted image showing subtle blurring of gray/white matter interface in the left superior frontal gyrus. (H) Intracranial ictal EEG showed fast activity (~80Hz [yellow]) and repetitive spiking (red oval outline) over the superior frontal gyrus. (I) Resected specimen from the seizure onset zone was unremarkable apart from meningeal congestion and is shown in postfixation 5-mm slices in (J) through the main sulcus. (K) A 9.4 Tesla (T) MRI was performed on the fixed tissue slice shown in (J) overnight using 9.4T MR scanner (Agilent Technologies, Santa Clara, CA) with sequences including T2 (as shown in K) that showed ill-defined mild blurring of the cortex and white matter in the depths of the sulcus at the deep resection margin (K, arrow), which corresponded to the region with localized dysmorphic neurones with excess lipofuscin and dyslamination on histology, as shown in (L), from the same region with neuronal nuclei (NeuN) and SMI32 immunolabeling. This case has been reported in a previous study of quantitative MRI analysis in epilepsy resections (Reeves et al, Brain Pathology, 2015). Bar in (I) is equivalent to 1cm.

Proteomics Analysis

This was carried out on 2 cases with FNL (E1, E2), 2 pathology-negative cases (E8, E13), and 1 FCDIIB case (E19). One hundred fifty-nine proteins were identified in the proteomes of neurones in cases with FNL and pathology-negative cases. Expression of 76 proteins was found to be higher in DN/L in cases with FNL compared to neurones in pathology-negative cases (fold change, >1; Fig 3A–D). Most of the upregulated proteins in FNL cases were intracellular proteins, found in membrane-bounded organelles and vesicles. Twenty-four of the upregulated proteins in cases with FNL were lipofuscin-related proteins, which had been reported in a previous proteomic study that had extracted 49 major lipofuscin proteins from brain samples of a 64-year-old patient with Alzheimer's disease (AD) with Braak stage IV and Consortium to Establish a Registry for Alzheimer's Disease (CERAD) grade C and 2 normal aging donors of 85 (Braak I, CERAD grade 0) and 83 years (Braak II, CERAD grade 0).[23] This supported the impression of an excess of lipofuscin-related proteins in FNL. Upregulated proteins in FNL cases were noted to involve various pathways identified from pathway databases ($p < 0.01$). In particular, clathrin, dynamin-1, adaptor protein-2 (AP2), synapsin, syntaxin, synaptotagmin, and vesicle-associated membrane proteins are involved in synaptic clathrin-mediated vesicle pathways ($p = 0.004$; Fig 3D), which have roles in autophagy, phagosome, and lysosomal pathways.[24,25] In contrast, these vesicle-associated proteins showed either no changes or fold decrease in FCDIIB compared to pathology-negative cases.

Further immunohistochemistry was carried out for clathrin and dynamin-1 in all cases with FNL, and pathology-negative (E7–E9) and FCDIIB cases (E13 and E17–E18; Fig 4A–I). Using anti-clathrin antibodies specific for the c-terminus of the heavy chain (Fig 4), strong granular immunopositivity was observed in the cytoplasm and axon hillocks of the majority of DN/L in cases with FNL, with a similar distribution to PAS (Fig 4A). There were minor degrees of cytoplasmic positivity for clathrin in neurones in pathology-negative cases (Fig 4D). In FCDIIB cases, very sparse clathrin-labeled DN were observed (Fig 4F), and focal granular clathrin labeling of balloon cells, often distributed at the margins of the cytoplasm, was also noted (Fig 4G). Anti-dynamin-1, specific for the c-terminus of dynamin-1, showed variable labeling in cases with FNL, with some unlabeled DN/L, whereas the majority showed cytoplasmic positivity (Fig 4B–C). Normal-appearing cortical neurones, including interstitial white matter neurones of normal morphology, were diffusely positive for dynamin-1 in pathology-negative cases (Fig 4E). The DN in FCDIIB cases showed mainly intense cytoplasmic labeling (Fig 4H), but balloon cells were strikingly negative, for dynamin-1 (Fig 4I).

Clinical Investigations and Outcome

A review of clinical data (Supplementary Table 1) revealed no significant difference in mean age of onset of epilepsy in cases with FNL (11.8 years) compared to pathology-negative (8 years) and FCDIIB cases (9.2 years; $p = 0.29$). Mean age at surgery was between 30 and 31 years in all three pathology groups. A family history of epilepsy in a first-degree relative was noted in 3 of 6 cases with FNL, but in none of the pathology-negative or FCDIIB cases. The preoperative MRI was abnormal in 5 of 6 cases with FNL, with subtle abnormalities in the cortical/white matter interface and blurring of the boundaries and cortical signal change (Supplementary Table 1; Fig 5). In contrast, only 2 of 7 pathology-negative cases showed any cortical MRI abnormality, whereas 5 of 7 FCDIIB cases were abnormal, showing MRI features typical of FCDIIB, including the hallmark "transmantle" sign, in 2 cases (E18 and E19). IC-EEG recordings, using depth electrodes and/or subdural strips or grids, had been carried out preoperatively in all 20 cases, and in the majority of cases, separate samples were resected from regions of different activity including: (1) seizure focus/onset zone and (2) regions of secondary involvement (early and late spreading zones; Supplementary Table 1). DN/L were noted in samples from the seizure onset site in 5 of 6 cases with FNL and also in regions with secondary EEG involvement in 2 cases. There was no significant difference in postoperative outcomes between the three groups, with 2 of 6 patients seizure free in the FNL group, compared to 6 of 7 in FCDIIB and 2 of 7 in the pathology-negative group ($p = 0.073$), but this is a small series. It was not possible to comment on the completeness of resection in the majority of cases with FNL; in only 1 case with FNL (E3), the lesion was localized to the bottom of a sulcus and appeared to be completely resected during surgery, and this patient was seizure free postoperatively. There was no significant difference in the length of follow-up (range, between 2 and 6 years) between the three groups.

Discussion

We describe a novel neuropathological finding in young-adult patients with focal epilepsy localizing to the frontal lobe, characterized by excessive lipofuscin accumulation within dysmorphic-appearing neurones. The proteome of DN/L in cases with FNL compared to neurones in pathology-negative FLE cases revealed increased

lipofuscin-related proteins, comparable to the patterns noted in aged and AD human brains. FNL was typically associated with more-subtle cortical MRI abnormalities compared to FCDIIB, was present in the active seizure onset site, and was associated with a family history of epilepsy in half the cases. Although several histological features initially suggested a cortical dysplasia, this pathology appeared distinct from FLE with typical FCDIIB. We propose that this represents a distinct neuronal pathology in focal epilepsy involving the frontal lobe and is secondary to enhanced cellular autophagy.

FNL Is Distinct From FCDIIA and IIB

FCDIIB more commonly arises in the frontal lobes based on ascertainment from epilepsy surgical series.[26] Hallmark features typical of FCDIIB (presence of balloon cells and dysmorphic neurones) were also observed in one third of our FLE patients. Although no frontal FCDIIA cases were present in this series, a comparison with FCDIIA from other regions was made. Several lines of evidence in our study suggest that FNL is a distinct pathology from FCDIIA and IIB: (1) presence of excess neuronal lipofuscin (confirmed through histological stains, electron and fluorescent microscopy, proteomics where possible), which was not evident in FCDIIA and IIB or pathology-negative cases, despite patients having similar ages and duration of epilepsy; (2) ring-like rearrangement of neurofilaments in DN/L surrounded the accumulation of lipofuscin and was never observed in DN of FCDIIA and IIB (but we have observed this in neuronal storage disorders (as illustrated in Fig 2L); (3) DN/L of FNL cases were confined to the cortical layers and did not "trail" into the underlying white matter, unlike FCDIIA and IIB; (4) expression patterns of ubiquitin, p62, clathrin, and dynamin-1 were different in abnormal cell types in FNL compared to FCDIIB cases; and (5) a suggestion of different clinical features in this new pathology, with MRI features being more subtle in cases with FNL compared to typical FCDIIB, and an impression of better postoperative seizure control in FCDIIB (based on this current small series as well as the literature[9]), with 86% of FCDIIB cases becoming seizure free compared to 33% of cases with FNL. Furthermore, there were no "overlap" cases to suggest that cases with FCDIIB will accumulate FNL over time or that cases with FNL will develop FCDIIB.

Abnormal Autophagic and mTOR Pathways in FNL

Lipofuscin is composed of approximately two thirds proteins, one third lipid, and a small amount of carbohydrates and metals.[27] Though the number of cases in this analysis is small, with the possible exclusion of some proteins insoluble to trypsin digestion, our proteomic studies nevertheless revealed an upregulation of lipofuscin-related proteins in the DN/L in cases with FNL, reinforcing findings in our immunohistochemical and EM studies. Previous proteomic studies of lipofuscin in the postmortem aging human brain (from the ninth decade) detected abnormalities of mitochondrial, cytoskeletal, and membranous proteins.[23] Consistently, these proteins were also observed in high levels in our proteomic analysis of DN/L in cases with FNL, and yet these patients in our series were only in their third to fourth decades. Thus, the advanced accumulation of lipofuscin in DN/L of young patients with FNL appears not to be age related, but disease linked. Lipofuscin accumulation is a normal physiological process of the aging cell,[28] where accumulation is attributed to incomplete digestion of proteins and lipids over the cell life span. However, upregulation of lipofuscin-related proteins in young patients with FNL in this study may be attributed to impairments to the autophagic pathway. Autophagy in normal cellular homeostasis enables removal or recycling of damaged proteins and organelles and is an essential mechanism for cell survival.[29] Impaired autophagy is implicated in several neurodegenerative diseases.[32] p62 is an ubiquitin-binding protein and a substrate of autophagy, and its levels are inversely associated with autophagy flux.[30,31] In this study, we observed infrequent labeling of DN/L with p62 in cases with FNL, in contrast to the frequent strong expression in abnormal cells of FCDIIB cases. These findings are consistent with previous studies, which reported p62 labeling in the nucleus of balloon cells, but not DN, and absent ubiquitin expression in balloon cells,[22] and another study, which reported nuclear and cytoplasmic p62 labeling in both balloon cells and DN in FCDIIB, colocalizing with ubiquitin.[32] These observations support impaired autophagy cellular mechanisms operating in FCDIIB, in contrast to evidence for enhanced autophagy flux, resulting in excess lipofuscin accumulation, in cases with FNL (Fig 6).

mTOR is a nutrient-responsive kinase, and it is one of the major inhibitors of autophagy.[28] When the intracellular concentrations of growth factors/nutrients (carbohydrate, amino acid, and adenosine triphosphate [ATP]) are high, the mTOR pathway is activated and autophagy is inhibited: mTOR complex 1 (mTORC1) will phosphorylate the transcription factor, TFEB, to prevent its translocation to the nucleus. Conversely, during starvation, mTORC1 is inhibited, to allow autophagy to begin; but during prolonged starvation, mTORC1 is reactivated and autophagic lysosome reformation (ALR) is initiated.[33] mTOR pathway dysregulation is well recognized in

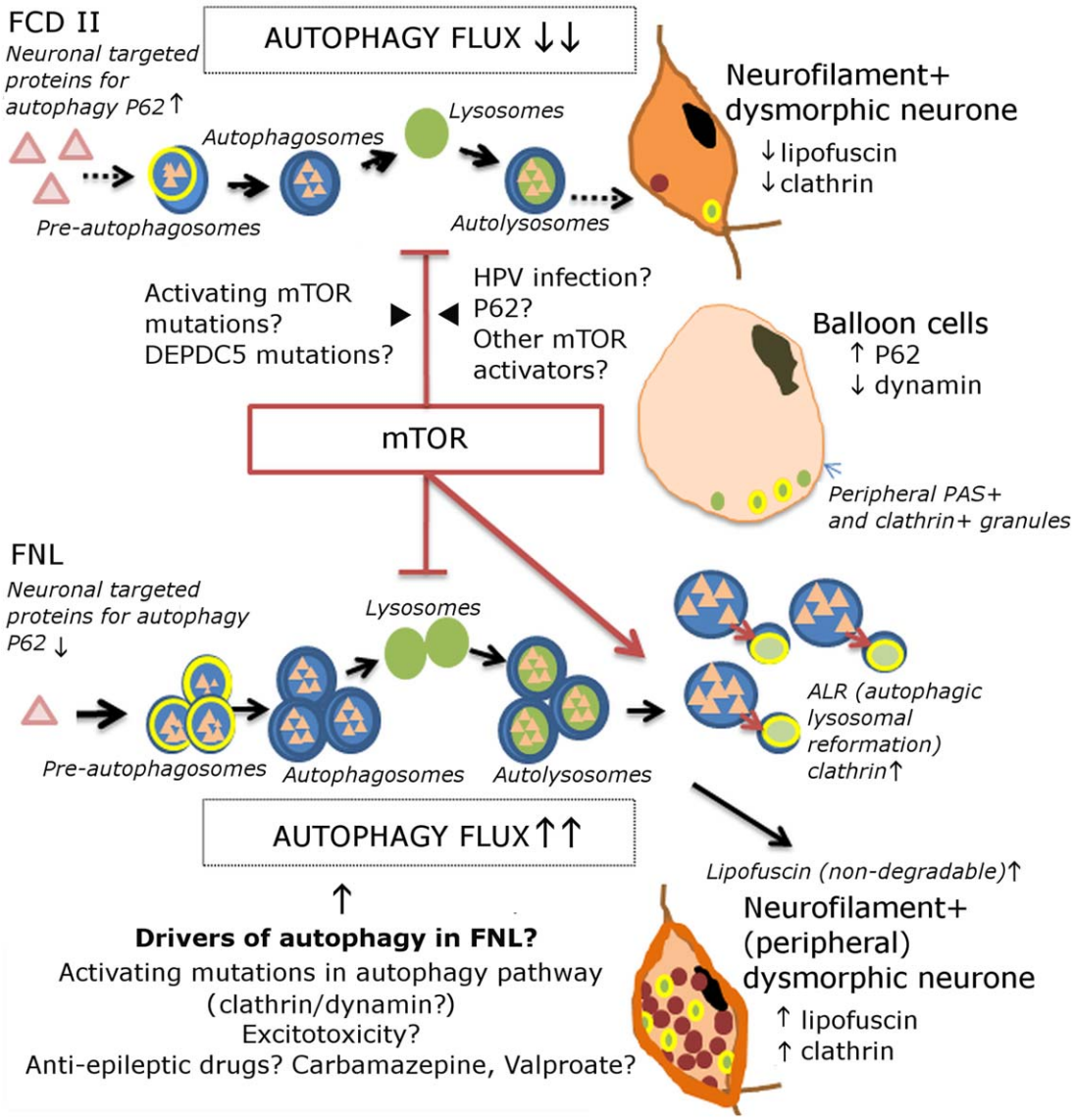

FIGURE 6: Possible pathways of abnormal autophagy in cases with frontal lobe epilepsy case with excess neuronal lipofuscin (FNL) compared to frontal cortial dysplasia type IIB (FCDIIB). Normally, inactivation of mammalian target of rapamycin (mTOR) activity leads to lysosomal biogenesis and autophagy, a process where autophagosomes fuse with lysosomes to degrade intracellular materials. In FCDIIB, there is mTOR activation with resultant suppression of autophagy (top row). In FNL, despite mTOR activation, there is enhanced autophagy. mTOR, in this pathology, may enhance the process of autophagy lysosome reactivation (ALR), which is clathrin dependent, leading to excess cellular clathrin as well as prolonging inhibition of autophagy, resulting in accumulation of nondegraded materials at various stages of autophagy or ALR processes, thus increasing formation of lipofuscin. Clathrin-coated vesicles and trafficking (yellow); lysosomes (green); lipofuscin cellular accumulation (dark red); and cytoplasmic neurofilaments (orange). PAS = periodic acid–Schiff.

FCD and in tubers.[34,35] Elevated expression of pS6 and other phosphoproteins in the mTOR pathway has been reported in DN and balloon cells of FCDIIB patients.[18,36–38] More recently, activating somatic mutations in *MTOR* have been shown in FCDIIA and IIB cases,[10,12] and *DEPDC5* mutations have been reported in familial cases of FCDIIA.[39] Activation of mTOR has also been more widely implicated in different epilepsy pathologies[18] and epileptogenic mechanisms.[40] In this study, we again utilized pS6 as a reliable marker of the activated mTOR pathway,[36] and the strong immunoreactivity for pS6 supported mTOR pathway activation in the DN/L of cases with FNL. In general, we observed less labeling in the abnormal cell types of cases with FNL for DEPDC5 protein compared to labeling observed in FCDIIB, suggesting differences in pathway activation. In FCDIIB, the net effect of mTOR activation is suppression of autophagy,[22] but this appears to be overridden in cases with FNL by as-yet unidentified drivers of autophagy (Fig 6). Future genetic studies will need

to be conducted to determine whether there are any specific mutations directly driving mTOR pathway activation in FNL.

Evidence for Abnormal Clathrin-Mediated Vesicle Formation and Trafficking in FNL

Proteomic studies showed that DN/L in cases with FNL had higher amounts of clathrin and its interacting proteins compared to pathology-negative cases. Elevated clathrin levels have previously been reported in the normal aged human brain.[23] We confirmed this finding with immunohistochemistry, which showed prominent labeling of DN/L with anticlathrin antibodies compared to normal neurones and DN in FCDIIB, with only focal, marginal labeling of balloon cells noted. Clathrin and its adaptor proteins regulate receptor-mediated endocytosis by stabilizing the small invaginations of the plasma membrane used to retrieve or absorb specific membranous ligands and receptors. Clathrin is integral to the formation of the preautophagosome in autophagy,[41] to neurotransmitter recycling at the nerve terminal[42,43] as well as during ALR, where tubules and vesicles are extruded from autolysosomes in a clathrin- and phosphatidylinositol-4,5-bisphosphate–dependent manner to reform lysosomes.[25,44] Expression of clathrin on mature lysosomes has previously been reported, and it is believed that this interaction facilitates the retrograde transport of materials out of the lysosomes to maintain homeostasis.[45] The increased cellular expression of clathrin in cases with FNL may mark the presence of increased numbers of unprocessed clathrin-containing preautophagosomes, or autophagosomes, or the clustering of clathrin on lysosomes (following ALR and lysosomal retrograde transport) as a result of prolonged autophagy attenuation in DN/L (Fig 6). Clathrin dysregulation may be pivotal to the observed cytopathology in cases with FNL and, given that clathrin-mediated endocytosis is also involved in neurotransmitter trafficking at the presynaptic terminal, fluxes in cellular levels could potentially influence neuronal activity and have a direct role in excitability.

Dynamin-1 is a central nervous system–specific GTPase essential for clathrin-mediated endocytosis and vesicle trafficking. Dynamin-1 protein was also increased in protein fractions of cases with FNL. Dynamin-1 also has roles in autophagic pathways and activity-dependent synaptic vesicle recycling.[46] Intriguingly, cytoplasmic negativity was observed in a subpopulation of DN/L cells, as well as striking negativity in balloon cells, which could indicate a specific cellular dysfunction of dynamin-1 linking these pathologies. Genetic mutations of *DNM1*, which encodes dynamin-1, have been recently recognized in epileptic encephalopathies[47] and cause epilepsy in experimental models[48,49] and further investigation in cases with FNL and FCDIIB is warranted.

In conclusion, we have identified a novel neuropathological abnormality in FLE patients, mimicking a cortical dysplasia, but distinct, from recognised types of FCDIIA or IIB, as supported by histological and proteomics analysis. We have demonstrated abnormalities in autophagic pathways, which have likely resulted in the observed neuronal dysmorphism. The findings from this study have highlighted a family history in cases with FNL, which could signify an underlying genetic predisposition to FNL. Future work will be directed to identify candidate genes/pathways. This study also identifies further lines of investigation of genes regulating autophagy and vesicle trafficking that may underpin this pathology, its contribution to epileptogenesis, and lead to identification of novel therapeutic targets.

Acknowledgment

This work is supported by the Medical Research Council (grant MR/JO127OX/1). This work was undertaken at UCLH/UCL who received a proportion of funding from the Department of Health's NIHR Biomedical Research Centres funding scheme. Z.M. received funding from the European Union Seventh Framework Programme (FP7/2007-2013) under grant agreement EPITARGET, #602102. The Epilepsy Society Brain and Tissue Bank at UCL is funded by the Epilepsy Society.

We are grateful to Tom Jacques and Glen Anderson for their help with EM in case E1 and Ernestas Sirka for his help with proteomic analyses.

Author Contributions

J.L., M.T., and S.S. were involved in the conception and design of the study and the drafting of the manuscript and figures. C.R., M.G., Z.M., and M.Ta. were involved in neuropathology experiments and interpretation. B.D., A.C., A.M., A.W.M., A.A., C.H., and S.A. are clinicians and neuroradiologists involved in the interpretation and evaluation of MRI and clinical data in this study. K.M. was involved in the proteomic analyses and interpretation of the data.

Potential Conflicts of Interest

Nothing to report.

References

1. Boillot M, Baulac S. Genetic models of focal epilepsies. J Neurosci Methods 2015;260:132–43.
2. Baulac S. Genetics advances in autosomal dominant focal epilepsies: focus on DEPDC5. Prog Brain Res 2014;213:123–39.

3. Scheffer IE, Heron SE, Regan BM, et al. Mutations in mammalian target of rapamycin regulator DEPDC5 cause focal epilepsy with brain malformations. Ann Neurol 2014;75:782–7.
4. Baulac S, Ishida S, Marsan E, et al. Familial focal epilepsy with focal cortical dysplasia due to DEPDC5 mutations. Ann Neurol 2015;77:675–83.
5. D'Gama AM, Geng Y, Couto JA, et al. Mammalian target of rapamycin pathway mutations cause hemimegalencephaly and focal cortical dysplasia. Ann Neurol 2015;77:720–5.
6. Kuzniecky R. Epilepsy and malformations of cortical development: new developments. Curr Opin Neurol 2015;28:151–7.
7. Jamuar SS, Walsh CA. Genomic variants and variations in malformations of cortical development. Pediatr Clin North Am 2015;62: 571–85.
8. Taylor DC, Falconer MA, Bruton CJ, et al. Focal dysplasia of the cerebral cortex in epilepsy. J Neurol Neurosurg Psychiatry 1971; 34:369–87.
9. Guerrini R, Duchowny M, Jayakar P, et al. Diagnostic methods and treatment options for focal cortical dysplasia. Epilepsia 2015; 56:1669–86.
10. Lim JS, Kim WI, Kang HC, et al. Brain somatic mutations in MTOR cause focal cortical dysplasia type II leading to intractable epilepsy. Nat Med 2015;21:395–400.
11. Nakashima M, Saitsu H, Takei N, et al. Somatic Mutations in the MTOR gene cause focal cortical dysplasia type IIb. Ann Neurol 2015;78:375–86.
12. Leventer RJ, Scerri T, Marsh AP, et al. Hemispheric cortical dysplasia secondary to a mosaic somatic mutation in MTOR. Neurology 2015;84:2029–32.
13. Blümcke I, Thom M, Aronica E, et al. The clinicopathologic spectrum of focal cortical dysplasias: A consensus classification proposed by an ad hoc Task Force of the ILAE Diagnostic Methods Commission1. Epilepsia 2011;52:158–74.
14. Krsek P, Maton B, Korman B, et al. Different features of histopathological subtypes of pediatric focal cortical dysplasia. Ann Neurol 2008;63:758–69.
15. Kim DW, Lee SK, Chu K, et al. Predictors of surgical outcome and pathologic considerations in focal cortical dysplasia. Neurology 2009;72:211–6.
16. Duncan J, Winston G, Koepp M, et al. Brain imaging in the assessment for epilepsy surgery. Lancet Neurol 2016;15:420–33.
17. Nowell M, Sparks R, Zombori G, et al. Comparison of computer-assisted planning and manual planning for depth electrode implantations in epilepsy. J Neurosurg 2016;124:1820-1828.
18. Liu J, Reeves C, Michalak Z, et al. Evidence for mTOR pathway activation in a spectrum of epilepsy-associated pathologies. Acta Neuropathol Commun 2014;2:71.
19. Heywood WE, Mills P, Grunewald S, et al. A new method for the rapid diagnosis of protein N-linked congenital disorders of glycosylation. J Proteome Res 2013;12:3471–3479.
20. Benavides SH, Monserrat AJ, Fariña S, et al. Sequential histochemical studies of neuronal lipofuscin in human cerebral cortex from the first to the ninth decade of life. Arch Gerontol Geriatr 2002;34:219–231.
21. Boellaard JW, Schlote W. Ultrastructural heterogeneity of neuronal lipofuscin in the normal human cerebral cortex. Acta Neuropathol 1986;71:285–294.
22. Yasin SA, Ali AM, Tata M, et al. mTOR-dependent abnormalities in autophagy characterize human malformations of cortical development: evidence from focal cortical dysplasia and tuberous sclerosis. Acta Neuropathol 2013;126:207–218.
23. Ottis P, Koppe K, Onisko B, et al. Human and rat brain lipofuscin proteome. PROTEOMICS 2012;12:2445–2454.
24. Behrends C, Sowa ME, Gygi SP, et al. Network organization of the human autophagy system. Nature 2010;466:68–76
25. Rong Y, Liu M, Ma L, et al. Clathrin and phosphatidylinositol-4,5-bisphosphate regulate autophagic lysosome reformation. Nat Cell Biol 2012;14:924–934.
26. Love S, Budka H, Ironside J, et al. In: Epilepsy. Greenfield's Neuropathology, Ninth Edition, Vol. 2, CRC Press, Taylor & Francis Group, Boca Raton, Florida, 2015, 1961 pp.
27. Brunk UT, Terman A. Lipofuscin: mechanisms of age-related accumulation and influence on cell function. Free Radic Biol Med 2002;33:611–619.
28. Sulzer D, Mosharov E, Talloczy Z, et al. Neuronal pigmented autophagic vacuoles: lipofuscin, neuromelanin, and ceroid as macroautophagic responses during aging and disease. J Neurochem 2008;106:24–36.
29. Marino G, Madeo F, Kroemer G. Autophagy for tissue homeostasis and neuroprotection. Curr Opin Cell Biol 2011;23: 198–206.
30. Komatsu M, Kominami E, Tanaka K. Autophagy and Neurodegeneration. Autophagy 2006;2:315–317.
31. Ichimura Y, Komatsu M. Selective degradation of p62 by autophagy. Semin Immunopathol 2010;32:431–436.
32. Iyer A, Prabowo A, Anink J, et al. Cell injury and premature neurodegeneration in focal malformations of cortical development. Brain Pathol 2014;24:1–17.
33. Zhou J, Tan S-H, Nicolas V, et al. Activation of lysosomal function in the course of autophagy via mTORC1 suppression and autophagosome-lysosome fusion. Cell Res 2013;23:508–523.
34. Miyahara H, Natsumeda M, Shiga A, et al. Suppressed expression of autophagosomal protein LC3 in cortical tubers of tuberous sclerosis complex. Brain Pathol 2013;23:254–262.
35. Marin-Valencia I, Guerrini R, Gleeson JG. Pathogenetic mechanisms of focal cortical dysplasia. Epilepsia 2014;55:970–978.
36. Baybis M, Yu J, Lee A, et al. mTOR cascade activation distinguishes tubers from focal cortical dysplasia. Ann Neurol 2004;56: 478–487.
37. Ljungberg MC, Bhattacharjee MB, Lu Y, et al. Activation of mammalian target of rapamycin in cytomegalic neurons of human cortical dysplasia. Ann Neurol 2006;60:420–429.
38. Lin YX, Lin K, Kang DZ, et al. Similar PDK1–AKT–mTOR pathway activation in balloon cells and dysmorphic neurons of type II focal cortical dysplasia with refractory epilepsy. Epilepsy Res 2015;112: 137–149.
39. Scerri T, Riseley JR, Gillies G, et al. Familial cortical dysplasia type IIA caused by a germline mutation in DEPDC5. Ann Clin Transl Neurol 2015;2:575–580.
40. Meng XF, Yu JT, Song JH, et al. Role of the mTOR signaling pathway in epilepsy. J Neurol Sci 2013;332:4–15.
41. Ravikumar B, Moreau K, Jahreiss L, et al. Plasma membrane contributes to the formation of pre-autophagosomal structures. Nat Cell Biol 2010;12:747–757.
42. Brodin L, Low P, Shupliakov O. Sequential steps in clathrin-mediated synaptic vesicle endocytosis. Curr Opin Neurobiol 2000; 10:312–320.
43. Yao PJ, O'Herron TM, Coleman PD. Immunohistochemical characterization of clathrin assembly protein AP180 and synaptophysin in human brain. Neurobiol Aging 2003;24:173–178.
44. Yu L, McPhee CK, Zheng L, et al. Termination of autophagy and reformation of lysosomes regulated by mTOR. Nature 2010;465: 942–946.
45. Traub LM, Bannykh SI, Rodel JE, et al. AP-2-containing clathrin coats assemble on mature lysosomes. J Cell Biol 1996;135:1801–1814.

46. Royle SJ, Lagnado L. Clathrin-mediated endocytosis at the synaptic terminal: bridging the gap between physiology and molecules. Traffic 2010;11:1489–1497.

47. EuroEPINOMICS-RES Consortium; Epilepsy Phenome/Genome Project; Epi4K Consortium. De novo mutations in synaptic transmission genes including DNM1 cause epileptic encephalopathies. Am J Hum Genet 2014;95:360–370.

48. Boumil RM, Letts VA, Roberts MC, et al. A missense mutation in a highly conserved alternate exon of dynamin-1 causes epilepsy in fitful mice. PLoS Genet 2010;6:e1001046.

49. Asinof SK, Sukoff Rizzo SJ, Buckley AR, et al. Independent neuronal origin of seizures and behavioral comorbidities in an animal model of a severe childhood genetic epileptic encephalopathy. PLoS Genet 2015;11:e1005347.